# Measurement and modeling of uniaxial and planar extensional viscosities for linear isotactic polypropylenes ⓕ

ⓘD Jiri Drabek and ⓘD Martin Zatloukal

**COLLECTIONS**

Note: This paper is part of the special topic, One Hundred Years of Giesekus.

ⓕ  This paper was selected as Featured

View Online   Export Citation   CrossMark

---

**ARTICLES YOU MAY BE INTERESTED IN**

Prevention of edge fracture using a nontoxic liquid metal sealant
Physics of Fluids **35**, 011704 (2023); https://doi.org/10.1063/5.0135554

Knowledge discovery with computational fluid dynamics: Supercritical airfoil database and drag divergence prediction
Physics of Fluids **35**, 016113 (2023); https://doi.org/10.1063/5.0130176

Dissipation-optimized proper orthogonal decomposition
Physics of Fluids **35**, 015131 (2023); https://doi.org/10.1063/5.0131923

**Physics of Fluids**

Special Topic: Paint and Coating Physics

**Submit Today!**

AIP Publishing

**35**, 013105

# Measurement and modeling of uniaxial and planar extensional viscosities for linear isotactic polypropylenes Ⓕ

View Online    Export Citation    CrossMark

Jiri Drabek ⓘD and Martin Zatloukal[a) ] ⓘD

## AFFILIATIONS

Polymer Centre, Faculty of Technology, Tomas Bata University in Zlin, Vavreckova 5669, 760 01 Zlin, Czech Republic

Note: This paper is part of the special topic, One Hundred Years of Giesekus.
[a) ]Author to whom correspondence should be addressed: mzatloukal@utb.cz

## ABSTRACT

In this work, novel rectangular and circular orifice (zero-length) dies were used to measure planar and uniaxial extensional viscosities as a function of strain rate for various linear isotactic polypropylene melts by using Cogswell methodology. The obtained experimental data were combined with shear and uniaxial extensional viscosity data determined at very high strain rates. The ability of the molecularized generalized Newtonian fluid (mGNF) [M. Zatloukal and J. Drabek, "Generalized Newtonian fluid constitutive equation for polymer liquids considering chain stretch and monomeric friction reduction for very fast flows modeling," Phys. Fluids **33**(8), 083106 (2021)], Giesekus, and explicit Yao constitutive equations to describe the measured data was tested. It has been shown that including the effect of the chemical environment (i.e., the role of the oligomeric solvent) using a simplified version of the mGNF constitutive equation (instead of the commonly used Newton's law) can significantly improve the ability of the Giesekus and Yao viscoelastic constitutive equations to describe the measured experimental data, especially at very high strain rates with using adjustable parameters with a clear physical meaning.

## I. INTRODUCTION

Planar extension flow is when the polymer melt stretches in one direction, shrinks in the thickness direction, and has no shrinkage in the width direction. The extrusion film casting process is an energy storage membrane manufacturing technology in which planar stretching is important because it determines the polymer flow inside the flat dies and controls the unwanted neck-in phenomenon.[1–4] In more detail, it was found that the neck-in depends on the ratio of planar and uniaxial extensional viscosity.[5–8] While uniaxial extensional viscosity is a material property that can be relatively easily measured using a variety of experimental techniques,[9–12] determining planar extensional viscosity is one of the most challenging rheological tasks because of the difficulty of generating and controlling planar extensional flow. It is therefore not surprising that the planar extensional viscosity is not correctly handled when modeling polymer processing, and the flow phenomena associated with this material property are not yet fully understood. The objective of this work is to first use new rectangular[13,14] and circular orifice (zero-length) dies[15,16] to measure uniaxial and planar extensional viscosities for various polypropylene melts

using the Cogswell model[14,17,18] at medium strain rates and combine them with very-high-strain-rate-dependent shear and uniaxial extensional viscosities taken from our previous work.[19–22] Second, we assess the ability of the recently proposed molecularized generalized Newtonian fluid (mGNF),[23,24] Giesekus,[25–27] and recently proposed explicit Yao[28] constitutive equations to describe the shear and both extensional viscosities with a single set of parameters. Finally, we generalize Newton's law for the oligomeric solvent contribution to the stress tensor (i.e., to include the role of chemical environment) in the used viscoelastic constitutive equations to improve their behavior at very high strain rates.

## II. EXPERIMENTAL

Three linear isotactic polypropylenes (iPPs) Borflow HL504FB (76 k), HL508FB (64 k), and HL512FB (56 k) were used in this work. The molecular characteristics of the linear isotactic polypropylene melts used are summarized in Table I. Polypropylenes were characterized at 230 °C using a Rosand RH7-2 twin-bore capillary rheometer equipped with polyether ether ketone (PEEK) piston tips. Two circular

**TABLE I.** Basic characteristics of the isotactic polypropylenes used.

| Sample Name | $M_n$ (g mol$^{-1}$) | $M_w$ (g mol$^{-1}$) | $M_z$ (g mol$^{-1}$) | $M_{z+1}$ (g mol$^{-1}$) | $M_w/M_n$ (−) |
|---|---|---|---|---|---|
| HL504FB (76 k) | 17 200 | 75 850 | 165 500 | 278 000 | 4.41 |
| HL508FB (64 k) | 14 650 | 63 750 | 138 000 | 235 500 | 4.35 |
| HL512FB (56 k) | 14 250 | 56 250 | 114 500 | 187 500 | 3.95 |

dies with the same diameter of $D_d = 0.5$ mm but different length-to-diameter ratios, $L/D$, (0.12[14,29] and 16), and also two rectangular dies of width, $w = 10$ mm, gap size $h = 0.15$ mm and different $L/h$ ratios (0.12[14,29] and 16) were used to determine the uniaxial and planar extensional viscosities using the Cogswell model[14,17,18] (see Table II). In this table, $Q$ is the volumetric flow rate; $R$ is the radius of the capillary die; $w$ and $h$ are the width and gap size of the rectangular die, respectively; $L$ is the length of the long die; $P_{L,U}$ and $P_{L,P}$ are the pressure drop through the long die, which is circular and rectangular in shape, respectively; and $P_{0,U}$ and $P_{0,P}$ represent the entrance pressure drop measured on the circular and rectangular orifice die, respectively. The obtained data were combined together with shear and uniaxial extensional viscosity data determined at very high strain rates reported in our previous works.[19–22] The maximum Hencky strain, $\varepsilon_{max}$, achieved when measuring uniaxial and planar extensional viscosity during the abrupt contraction flow is given as

$$\varepsilon_{max} = \ln\left(\frac{A_b}{A_d}\right), \tag{1}$$

where $A_b$ and $A_d$ are the cross-sectional area of the barrel and the die, respectively.[30] The maximum Hencky strain for circular ($\varepsilon_{max,U}$) and rectangular ($\varepsilon_{max,P}$) orifice dies is then given as

$$\varepsilon_{max,U} = 2\ln\left(\frac{D_b}{D_d}\right), \tag{2}$$

$$\varepsilon_{max,P} = \ln\left(\frac{\pi D_b^2}{4wh}\right), \tag{3}$$

where $D_b$ is the barrel diameter (15 mm), $D_d$ is the orifice circular die diameter (0.5 mm), and $w$ and $h$ are the width (10 mm) and gap size (0.15 mm) of the rectangular orifice die. According to Eqs. (2) and (3), $\varepsilon_{max,U} = 6.8$ and $\varepsilon_{max,P} = 4.8$. Note that $\varepsilon_{max,U}$ is the same for uniaxial extensional viscosity measured at low strain rates (this work) and high strain rates (experimental data taken from our previous work[19–22]). It should also be mentioned that for the same volume flow rate and circular and rectangular die dimensions used, the Hencky strain, extensional strain rate (including wall shear rate and wall shear stress used in the Cogswell analysis) is smaller for planar extensional flow compared to uniaxial extensional flow. While maintaining the same volume flow rate in circular and rectangular geometries, the pressure measured on rectangular dies is much less compared to circle dies. Thus, given the limited resolution of pressure transducers, experimental data from rectangular dies are typically quantifiable at much higher volume flow rates compared to circular geometries.

## III. THEORETICAL

The following constitutive equations were chosen to describe the measured rheological data.

### A. Molecularized generalized Newtonian fluid model (mGNF)

A recently proposed molecularized generalized Newtonian fluid model was used in this work[23]

$$\underline{\underline{\tau}} = 2\eta\left(II_{\underline{\underline{D}}}, II_{\underline{\underline{\bar{L}}}}\right)\underline{\underline{D}}, \tag{4}$$

where $\underline{\underline{\tau}}$ stands for the extra stress tensor, $\underline{\underline{D}}$ represents the strain rate tensor, $\underline{\underline{\bar{L}}}$ is the objective velocity gradient (defined as $\underline{\underline{\bar{L}}} = \underline{\underline{L}} - \underline{\underline{\Omega}}$, where $\underline{\underline{L}}$ is velocity gradient and $\underline{\underline{\Omega}}$ is the tensor that gives the rate of rotation of the eigenvectors of $\underline{\underline{D}}$[31–35]) and $\eta(II_{\underline{\underline{D}}}, II_{\underline{\underline{\bar{L}}}})$ means the viscosity, which can vary with the second $II_{\underline{\underline{D}}} = 2tr(\underline{\underline{D}}^2)$ invariant of $\underline{\underline{D}}$ as well as on the second invariant of the objective velocity gradient $II_{\underline{\underline{\bar{L}}}} = 2tr(\underline{\underline{\bar{L}}}^2)$ according to Eq. (5) (note that $\underline{\underline{\bar{L}}}$ and the velocity gradient tensor $\underline{\underline{L}}$ are same in the steady-state flows[34,35])

**TABLE II.** A summary of the Cogswell model for the determination of uniaxial and planar extensional viscosities.[14,17,18]

| | Uniaxial extensional flow | Planar extensional flow |
|---|---|---|
| Apparent shear rate | $\dot{\gamma}_{app,U} = \dfrac{4Q}{\pi R^3}$ | $\dot{\gamma}_{app,P} = \dfrac{6Q}{wh^2}$ |
| Corrected shear stress | $\tau_{xy,corr,U} = \dfrac{(P_{L,U} - P_{0,U})R}{2L_U}$ | $\tau_{xy,corr,P} = \dfrac{(P_{L,P} - P_{0,P})h}{2L_P}$ |
| Apparent index of non-Newtonian behavior | $n_U = \dfrac{d\log(\tau_{xy,corr,U})}{d\log(\dot{\gamma}_{app,U})}$ | $n_P = \dfrac{d\log(\tau_{xy,corr,P})}{d\log(\dot{\gamma}_{app,P})}$ |
| Extensional stress | $\sigma_{E,U} = \dfrac{3}{8}(n_U + 1)P_{0,U}$ | $\sigma_{E,P} = \dfrac{1}{2}(n_P + 1)P_{0,P}$ |
| Extensional strain rate | $\dot{\varepsilon}_U = \dfrac{4\tau_{xy,corr,U}\dot{\gamma}_{app,U}}{3(n+1)P_{0,U}}$ | $\dot{\varepsilon}_U = \dfrac{2\tau_{xy,corr,P}\dot{\gamma}_{app,P}}{3(n+1)P_{0,P}}$ |
| Extensional viscosity | $\eta_{E,U} = \dfrac{\sigma_{E,U}}{\dot{\varepsilon}_U}$ | $\eta_{E,P} = \dfrac{\sigma_{E,P}}{\dot{\varepsilon}_P}$ |

$$\eta\left(II_{\underline{\underline{D}}}, II_{\underline{\underline{L}}}\right) = A^{1-f\left(II_{\underline{\underline{L}}}\right)} \eta\left(II_{\underline{\underline{D}}}\right)^{f\left(II_{\underline{\underline{L}}}\right)}. \tag{5}$$

Here, $\eta(II_{\underline{\underline{D}}})$ is given by the well-known Carreau–Yasuda model, Eq. (6), and $f(II_{\underline{\underline{L}}})$ varies between 1 ($II_{\underline{\underline{L}}} \to 0$) and 2 ($II_{\underline{\underline{L}}} \to \infty$) and is given by Eq. (7),

$$\eta\left(II_{\underline{\underline{D}}}\right) = \eta_\infty + \frac{\eta_0 - \eta_\infty}{\left[1 + \left(\lambda_1 \sqrt{II_{\underline{\underline{D}}}}\right)^a\right]^{\frac{1-n}{a}}}, \tag{6}$$

$$f\left(II_{\underline{\underline{L}}}\right) = \frac{2}{\left[\tanh\left(\lambda_2 \sqrt{II_{\underline{\underline{L}}}} + \beta\right)\right]^{\log_{\tanh(\beta)} 2}}. \tag{7}$$

Here, the parameters $\eta_0$ (zero-shear-rate viscosity), $\eta_\infty$ (infinite-shear-rate viscosity), $\lambda_1$ (reptation-mode relaxation time), $a$ (parameter characterizing transition from Newtonian to power-law regime), and $n$ (power-law index) are related to the shear viscosity curve while $\beta$ (extensional strain hardening parameter), $\lambda_2$ (Rouse mode relaxation time), and $A$ (parameter related to the asymptotic value for extensional viscosity, i.e., for $\dot{\varepsilon} \to \infty$) are obtained by fitting the steady-state extensional viscosity.

In pure shear flow

$$\underline{\underline{D}} = \frac{1}{2}\begin{pmatrix} 0 & \dot{\gamma} & 0 \\ \dot{\gamma} & 0 & 0 \\ 0 & 0 & 0 \end{pmatrix} \tag{8}$$

and

$$\underline{\underline{\bar{L}}} = \underline{\underline{L}} = \begin{pmatrix} 0 & \dot{\gamma} & 0 \\ 0 & 0 & 0 \\ 0 & 0 & 0 \end{pmatrix}, \tag{9}$$

and thus, $f(II_{\underline{\underline{L}}})$ defined by Eq. (7) becomes equal to 1 because $II_{\underline{\underline{L}}} = 0$; that is, the shear viscosity becomes dependent on the second invariant of the strain rate tensor only with $II_{\underline{\underline{D}}} = \dot{\gamma}^2$ as follows:

$$\eta(\dot{\gamma}) = \eta_\infty + \frac{\eta_0 - \eta_\infty}{\left[1 + (\lambda_1\dot{\gamma})^a\right]^{\frac{1-n}{a}}}. \tag{10}$$

In general steady-state extensional flow

$$\underline{\underline{D}} = \underline{\underline{\bar{L}}} = \underline{\underline{L}} = \dot{\varepsilon}\begin{pmatrix} 1 & 0 & 0 \\ 0 & m & 0 \\ 0 & 0 & -(1+m) \end{pmatrix}, \tag{11}$$

$$II_{\underline{\underline{D}}} = II_{\underline{\underline{\bar{L}}}} = II_{\underline{\underline{L}}} = 4\dot{\varepsilon}^2(m^2 + m + 1). \tag{12}$$

For simple uniaxial extensional flow $m = -0.5$, for a planar extensional flow $m = 0$, and for equibiaxial extensional flow, $m = 1$.[9] A combination of Eqs. (4)–(7), (11), and (12) leads to the following expression for the extensional viscosity:

$$\eta_E = 2(2+m)A^{1-f(\dot{\varepsilon})}\eta(\dot{\varepsilon})^{f(\dot{\varepsilon})}, \tag{13}$$

where

$$\eta(\dot{\varepsilon}) = \eta_\infty + \frac{\eta_0 - \eta_\infty}{\left[1 + \left(\lambda_1 2\dot{\varepsilon}\sqrt{m^2 + m + 1}\right)^a\right]^{\frac{1-n}{a}}} \tag{14}$$

and

$$f(\dot{\varepsilon}) = \frac{2}{\left[\tanh\left(\lambda_2 2\dot{\varepsilon}\sqrt{m^2 + m + 1} + \beta\right)\right]^{\log_{\tanh(\beta)} 2}}. \tag{15}$$

The asymptotic formula for extensional viscosity is given as

$$\eta_{E,\infty} = \lim_{\dot{\varepsilon} \to \infty} \eta_E = 2(2+m)\frac{\eta_\infty^2}{A}. \tag{16}$$

The constant $A$ can be expressed from Eq. (16) considering uniaxial extensional flow, that is $\eta_{E,U,\infty} = \lim_{\dot{\varepsilon} \to \infty} \eta_E(m = -0.5)$, as follows:

$$A = \frac{3\eta_\infty^2}{\eta_{E,U,\infty}}. \tag{17}$$

In this model, the expression for the uniaxial extensional viscosity at the high strain rate limit $\eta_{E,U,\infty}$ corresponds to the molecular expression for a fully extended Fraenkel chain[36] and is given by the following formula:[23]

$$\eta_{E,U,\infty} = 3\eta_0 \frac{\lambda_{\max}^2}{M_e} M_c^{x-1} M^{2-x}\left(\frac{\zeta_{\text{eq}}}{\zeta_{\text{aligned}}}\right)^{-1}, \tag{18}$$

where $M_e$ is the molar mass between entanglements, $\lambda_{\max}$ is the maximum chain stretch ratio, $M_c$ is the critical molar mass at which entanglements begin to occur, $M$ is the molar mass, $x$ represents the value by which the zero-shear rate viscosity, $\eta_0$, scales with $M^x$ above $M_c$ (typically $3.5 \pm 0.2$ for all linear and flexible molecules[37]), and $\frac{\zeta_{\text{eq}}}{\zeta_{\text{aligned}}}$ represents the ratio of monomeric friction coefficients for equilibrium and fully aligned chains. Alternatively, the parameter $A$ can also be determined from the known molecular parameters of the polymer melt by combining Eqs. (17) and (18) as follows:[23]

$$A = \frac{\eta_\infty^2}{\eta_0} \frac{M_e}{\lambda_{\max}^2} M_c^{1-x} M^{x-2} \frac{\zeta_{\text{eq}}}{\zeta_{\text{aligned}}}. \tag{19}$$

## B. Modified Giesekus model

The original Giesekus model has been proposed from a simple dumbbell theory for dilute solutions with the consideration of anisotropic drag.[25–27] The model is given as follows:

$$\underline{\underline{\tau}} = \underline{\underline{\tau}}_p + \underline{\underline{\tau}}_s, \tag{20}$$

$$\underline{\underline{\tau}}_p + \alpha\frac{\lambda}{\eta_p}\underline{\underline{\tau}}_p^2 + \lambda\overset{\triangledown}{\underline{\underline{\tau}}}_p = 2\eta_p\underline{\underline{D}}, \tag{21}$$

$$\underline{\underline{\tau}}_s = 2\eta_\infty\underline{\underline{D}}, \tag{22}$$

$$\eta_0 = \eta_\infty + \eta_p, \tag{23}$$

where $\underline{\underline{\tau}}$ is the extra-stress tensor, $\underline{\underline{\tau}}_p$ and $\underline{\underline{\tau}}_s$ are the polymer and solvent contribution to the stress tensor, $\eta_\infty$ is the solvent viscosity, $\eta_p$ is the polymer viscosity, $\eta_0$ is the zero-shear-rate viscosity, $\underline{\underline{D}}$ is the strain

rate tensor, $\lambda$ is the relaxation time, the symbol $\nabla$ represents the upper-convected time derivative, $G$ is the modulus, and $\alpha$ is the parameter characterizing anisotropic hydrodynamic drag. The minimum and maximum anisotropies correspond to $\alpha = 0$ and $\alpha = 1$, respectively.[38] The steady-state shear viscosity is given by the following equations:[39]

$$\eta = (\eta_\infty + \eta_p)\left[\frac{\eta_\infty}{\eta_p + \eta_\infty} + \left(1 - \frac{\eta_\infty}{\eta_p + \eta_\infty}\right)\frac{(1-f)^2}{1 + (1-2\alpha)f}\right], \quad (24)$$

$$f = \frac{1 - \chi}{1 + (1 - 2\alpha)\chi}, \quad (25)$$

$$\chi^2 = \frac{\left(1 + 16\alpha(1-\alpha)(\lambda\dot\gamma)^2\right)^{1/2} - 1}{8\alpha(1-\alpha)(\lambda\dot\gamma)^2}. \quad (26)$$

The steady-state extensional viscosity is given by the following equation:

$$\eta_E = 2(m+2)\eta_\infty + \frac{1}{2\alpha\dot\varepsilon}\frac{\eta_p}{\lambda}$$
$$\times\left\{\begin{array}{l} 2\dot\varepsilon\lambda(m+2) + \left[1 + 4\dot\varepsilon^2\lambda^2 + (8\alpha-4)\lambda\dot\varepsilon\right]^{1/2} \\ -\left[1 + 4\lambda^2(1+m)^2\dot\varepsilon^2 - 8\lambda\left(\alpha - \frac{1}{2}\right)(1+m)\dot\varepsilon\right]^{1/2} \end{array}\right\}. \quad (27)$$

It has been showed[40–43] that increasing the molecular weight of the oligomeric solvent leads to co-aligned orientation of short solvent molecules with long polymer chains, which reduces the monomeric friction coefficient and the extensional viscosity. In order to include this effect in viscoelastic models, let us assume that the solvent contribution to the stress tensor is given by the molecularized generalized Newtonian fluid model introduced in Sec. III A (with $\eta(II_{\underline{D}})$ being replaced by $\eta_\infty$ and $A$ replaced by $A_G$) as follows:

$$\underline{\tau}_s = 2A_G^{1-f\left(II_{\underline{L}}\right)}\eta_\infty^{f\left(II_{\underline{L}}\right)}\underline{D}. \quad (28)$$

In this case, the expression for shear viscosity remains unchanged (because $f(II_{\underline{L}})=1$), but the expression for extensional viscosity changes from Eq. (27) to the following expression:

$$\eta_E = 2(m+2)A_G^{1-f\left(II_{\underline{L}}\right)}\eta_\infty^{f\left(II_{\underline{L}}\right)} + \frac{1}{2\alpha\dot\varepsilon}\frac{\eta_p}{\lambda}$$
$$\times\left\{\begin{array}{l} 2\dot\varepsilon\lambda(m+2) + \left[1 + 4\dot\varepsilon^2\lambda^2 + (8\alpha-4)\lambda\dot\varepsilon\right]^{1/2} \\ -\left[1 + 4\lambda^2(1+m)^2\dot\varepsilon^2 - 8\lambda\left(\alpha - \frac{1}{2}\right)(1+m)\dot\varepsilon\right]^{1/2} \end{array}\right\}, \quad (29)$$

which gives the following asymptotic formula:

$$\eta_{E,\infty} = \lim_{\dot\varepsilon\to\infty}\eta_E = \frac{2(m+2)}{A_G}\eta_\infty^2 + \frac{2}{\alpha}\eta_p. \quad (30)$$

The constant $A_G$ can be expressed from Eq. (30) for the case of uniaxial extensional flow, that is, $\eta_{E,U,\infty} = \lim_{\dot\varepsilon\to\infty}\eta_E(m=-0.5)$, as follows:

$$A_G = \frac{3\eta_\infty^2}{\eta_{E,U,\infty} - \frac{2}{\alpha}\eta_p} = \frac{3\eta_\infty^2}{\eta_{E,U,\infty} - \frac{2}{\alpha}(\eta_0 - \eta_\infty)}. \quad (31)$$

Since $A_G$ is defined as a positive value, $\eta_{E,U,\infty} > \frac{2}{\alpha}(\eta_0 - \eta_\infty)$.

## C. Modified explicit Yao model

Yao proposed a constitutive equation in which the extra stress tensor is an explicit function of the objective velocity gradient with finite stretch and rotational recovery.[28] The model is based on a modified stress law for a general elastic material that includes finite stretch and disentanglement

$$\underline{\tau} = G\underline{B}^*, \quad (32)$$

$$G = G_0\xi^{-\psi}, \quad (33)$$

$$\xi = \frac{S_0}{S_0 + \lambda_0\sqrt{\frac{2}{3}tr\left(\underline{D}\cdot\underline{D}\right)}}, \quad (34)$$

$$\underline{B}^* = \left[\exp\left(\xi^{\alpha_0}n_0\lambda_0\underline{\bar{L}}\right)\cdot\exp\left(\xi^{\alpha_0}n_0\lambda_0\underline{\bar{L}}^T\right)\right]^{1/n_0}. \quad (35)$$

Here, $\underline{\tau}$ is the extra stress tensor, $G$ is the elastic modulus, $G_0$ is the initial elastic modulus ($G_0 = \frac{\eta_0}{\lambda_0}$), $\xi^{-\psi}$ represents the elastic modulus shape function controlled by the strain hardening coefficient $\psi$ ($0 \le \psi \le 1$)[35] taking into account the effect of finite chain stretch on the elastic modulus (i.e., that $G$ increases with increasing chain stretch), $S_0$ is the ceiling stretch (typically in the range of 1–3),[35] $\lambda_0$ is the relaxation time at small strain, $\underline{D}$ is the strain rate tensor, $\underline{B}^*$ is the generalized Finger tensor representing the accumulated elastic strain in the polymer melt considering both the effect of rotational relaxation controlled by index of rotational recovery $n_0$ ($1 \le n_0 \le 2$)[35] and the effect of the finite stretch on the relaxation time by using the shape function $\xi^{\alpha_0}$ controlled by the parameter $\alpha_0$ with a typical value around $1$[28] (i.e., a decrease in $\lambda_0$ with increased chain stretch), and $\underline{\bar{L}}$ is the objective velocity gradient. The explicit nature of the model represents the main advantage over previous implicit Yao models,[34,35] from which the current model is based. The explicit Yao model can be further generalized by including the solvent contribution via a molecularized Newtonian model (i.e., analogous to the modification describe above for the modified Giesekus model) to include the role of the chemical environment reported in Refs. 40–43, which leads to the following expression for the extra stress tensor:

$$\underline{\tau} = \frac{\eta_P}{\lambda_P}\xi^{-\psi}\left[\exp\left(\xi^{\alpha_0}n_0\lambda_P\underline{L}\right)\cdot\exp\left(\xi^{\alpha_0}n_0\lambda_P\underline{L}^T\right)\right]^{1/n_0}$$
$$+ 2A_Y^{1-f\left(II_{\underline{L}}\right)}\eta_\infty^{f\left(II_{\underline{L}}\right)}\underline{D}, \quad (36)$$

where $\xi$ is given by Eq. (34). The steady-state shear viscosity is given by the following equation:

$$\eta = \eta_p\frac{\xi^{-\psi}}{\lambda_p\dot\gamma}\frac{R^{2/n_0} - (4/R)^{2/n_0}}{2^{2/n_0}\sqrt{\gamma^2 + 4}} + \eta_\infty, \quad (37)$$

where $\xi = \frac{S_0}{S_0 + \frac{\lambda_P}{\sqrt{3}}\dot\gamma}$, $\gamma = \xi^{\alpha_0}n_0\lambda_P\dot\gamma$, and $R = \sqrt{4 + \gamma^2} + \gamma$.[28]

The steady-state extensional viscosity is given by the following equation:

$$\eta_E = \frac{\eta_p}{\lambda_p \dot{\varepsilon}} \xi^{-\psi} \left[ \exp\left( \xi^{\alpha_0} 2\lambda_p \dot{\varepsilon} \right) - \exp\left( -\xi^{\alpha_0} 2\lambda_p (1+m)\dot{\varepsilon} \right) \right]$$
$$+ 2(2+m) A_Y^{1-f(\dot{\varepsilon})} \eta_\infty^{f(\dot{\varepsilon})}, \tag{38}$$

where

$$\xi = \frac{S_0}{S_0 + 2\dot{\varepsilon}\lambda_P \sqrt{\dfrac{m^2 + m + 1}{3}}}. \tag{39}$$

The asymptotic formula for extensional viscosity is given as

$$\eta_{E,\infty} = \lim_{\dot{\varepsilon} \to \infty} \eta_E = 2(2+m) \frac{\eta_\infty^2}{A_Y}. \tag{40}$$

The constant $A_Y$ can be expressed from Eq. (40) considering uniaxial extensional flow, that is, $\eta_{E,U,\infty} = \lim_{\dot{\varepsilon} \to \infty} \eta_E (m = -0.5)$, as follows:

$$A_Y = \frac{3\eta_\infty^2}{\eta_{E,U,\infty}}. \tag{41}$$

As can be seen, the expression for the Yao model constant $A_Y$ is the same as for the mGNF model constant $A$ [compare Eqs. (17) and (41)]. Note that the original Yao's expressions for both viscosities are recovered if $\eta_\infty = 0$ (i.e., $\eta_p = \eta_0$ and $\lambda_P = \lambda_0$) in Eqs. (36)–(38). It should also be mentioned that the explicit Yao model is viscoelastic; that is, it can predict the first and second normal stress differences,[28] while the mGNF model cannot.

## IV. RESULTS AND DISCUSSION

Measured data for all three iPP samples combined with very-high-strain-rate-dependent shear and uniaxial extensional viscosities taken from our previous work[19–22] are shown in Figs. 1–3 together with the mGNF model (Fig. 1), the original and modified explicit Yao model (Fig. 2), and original and modified Giesekus model (Fig. 3). The corresponding model parameters are given in Tables III–VII.

The mGNF model has a high ability to describe all the measured rheological data shown in Fig. 1. Here, $\eta_0$, $\eta_\infty$, $\lambda_1$, $a$, and $n = 0$, $\eta_{E,U,\infty}$ parameters were taken from our previous work[19,21–23] and $\lambda_2$ and $\beta$ were determined from the fit of uniaxial and planar extensional viscosities (see Table III). As expected, the reptation-mode relaxation time $\lambda_1$ and Rouse mode relaxation time $\lambda_2$ increase with the weight-averaged molecular weight, $M_w$, while the extensional strain hardening parameter $\beta$ decreases with increasing $M_w$.[23,44]

A comparison between the single-mode Giesekus model predictions and the measured data is shown in Fig. 2 (left), and the corresponding model parameters are provided in Table IV. Also in this case, the parameters $\eta_0$ and $\eta_\infty$ were taken from our previous work[19,21–23] (i.e., the polymer viscosity $\eta_p$ is known in advance because $\eta_p = \eta_0 - \eta_\infty$). The remaining model parameters $\lambda$ and $\alpha$ were determined by fitting the measured strain-rate dependent shear, uniaxial, and planar extensional viscosities. As can be seen in Fig. 2 (left), the model captures the shape of shear viscosity vs shear rate, even when single-mode approach was used. However, the model is not able to describe the extensional strain thinning because it does not consider

the finite stretching of the polymer chains.[45–48] Weak extensional thinning in uniaxial extensional viscosity at moderate strain rates can only be achieved if $\alpha$ is sufficiently high. At very high extensional strain rates, the model predicts a constant extensional viscosity given as

$$\eta_{E,\infty} = 2(m+2)\eta_\infty + \frac{2}{\alpha}\eta_P. \tag{42}$$

The asymptotic formulas for the uniaxial and planar extensional viscosities for the case of the most extensional thinning (i.e., when $\alpha = 1$) are thus given as follows:

$$\eta_{E,U,\infty}(\alpha = 1) = 2\eta_0 + \eta_\infty, \tag{43}$$
$$\eta_{E,P,\infty}(\alpha = 1) = 2\eta_0 + 2\eta_\infty. \tag{44}$$

As can be seen, none of the above extensional viscosities ever drop below $2\eta_0 + \eta_\infty$. A closer analysis of Eq. (42) shows that the Giesekus model provides extensional thinning for uniaxial and planar extensional viscosity only when $2/3 < \alpha \le 1$ and $1/2 < \alpha \le 1$, respectively. The dependence of both extensional viscosities on the extensional strain rate for different values of $\alpha$ is shown in Fig. 4 using the parameters for the 76 k polypropylene melt. This explains why the Giesekus model is unable to describe the measured extensional strain thinning followed by extensional strain thickening in both extensional viscosities for the given iPP melts shown in Fig. 2 (left). On the other hand, the Giesekus's reptation-mode relaxation time $\lambda$ and the anisotropy parameter $\alpha$ (causing a decrease in $\eta_{E,\infty}$ as $\alpha$ increases) correctly increase with $M_w$ as expected.

The modified Giesekus model shows improved behavior in both extensional viscosities at very high extensional strain rates, as seen in Fig. 2 (right). The model describes extensional thinning for both extensional viscosities at moderate strain rates in the same way as the original Giesekus model (by setting $2/3 < \alpha \le 1$ with a minimum achievable uniaxial and planar extensional viscosity of $2\eta_0 + \eta_\infty$ and $2\eta_0 + 2\eta_\infty$, respectively), but it can also handle extensional strain hardening at very high strain rates (i.e., at values higher than the reciprocal value of the Rouse time) due to a modified expression for the solvent contribution to the stress tensor. The ability of the model to describe the extensional viscosities increases with the reduced $M_w$ of the tested iPPs, because in that case the minimum attainable extensional viscosities predicted by the original Giesekus model approach the experimentally determined minimum extensional viscosities. It is clear that the proposed modification of the "solvent" viscosity (to account for the effect of the chemical environment) can significantly improve the ability of the viscoelastic constitutive equations to describe the extensional rheology at very high strain rates. It should be mentioned that the behavior of the Giesekus model at moderate extensional strain rates can be further improved by modifying the expression for the polymer contribution to the stress tensor by incorporating the finite extensibility of the polymer molecules into dumbbell kinetic theory using the Peterlin approximation as shown in Refs. 45–48. The trend between the modified Giesekus's reptation-mode relaxation time $\lambda$ and $M_w$ remains the same as for the original Giesekus and mGNF models. Since $\lambda_2$ is of the same order as in the mGNF model, but its value increases (and does not decrease) with decreasing $M_w$, the $\lambda_2$ is also correlated with Rouse time in this case, but inversely. The effect of $M_w$ on the strain-hardening-related parameters $\alpha$ and $\beta$ is not clear in this case, as the ability of the modified
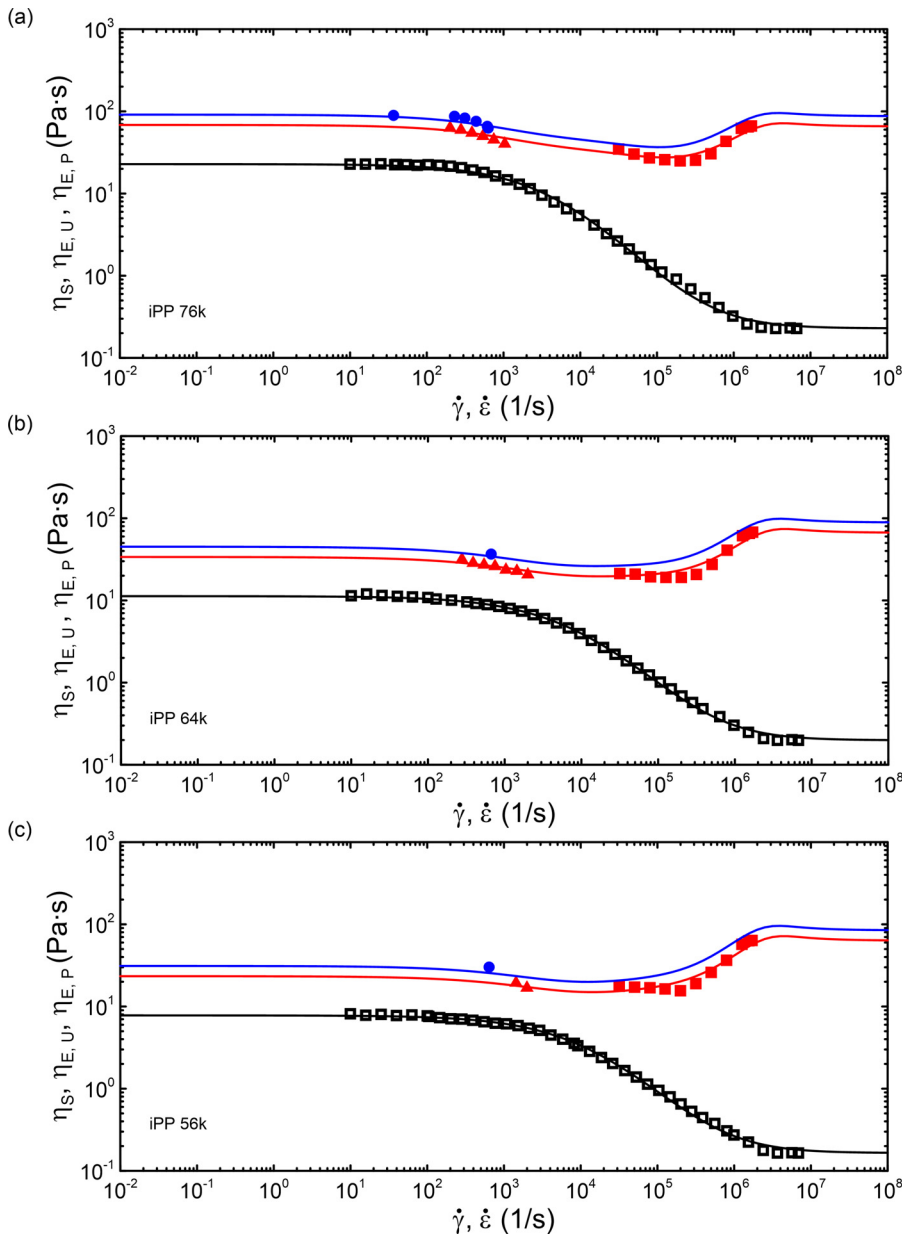
FIG. 1. Comparison between measured strain rate-dependent shear (open symbols), uniaxial (red full triangles and squares) and planar extensional viscosities (blue full circles), and mGNF model fits (curves) at $230\,^{\circ}C$ for three linear isotactic polypropylenes [76 k (a), 64 k (b), and 56 k (c)]. Here, $\eta_S$ is the shear viscosity, $\eta_{E,U}$ is the uniaxial extensional viscosity, $\eta_{E,P}$ is the planar extensional viscosity, $\dot{\gamma}$ is the shear rate, and $\dot{\varepsilon}$ is the extensional strain rate.

Giesekus model to fit the extensional viscosity data varies significantly with $M_w$ (the ability of the model to fit experimental data increases with reduced $M_w$, see Fig. 2 (right) and Table V for the fitting errors evaluated using the root mean square error, RMSE), which does not allow a direct physical interpretation of both parameters.

A comparison between the experimental data and the original explicit Yao model predictions is shown in Fig. 3 (left). As can be seen, the model is unable to describe the secondary Newtonian plateau in the shear viscosity curve, fails to describe the uniaxial viscosity data, and unrealistically predicts that the uniaxial and planar extensional viscosities cross each other at moderate strain rates and become infinite at very high strain rates. The corresponding model parameters

(six in total) are listed in Table VI, where $\eta_0$ was taken from Refs. 19 and 21–23 and the ceiling stretch $S_0$ was adjusted to 1 to ensure that model predicts extensional thinning at moderate strain rates[35] (which is typical flow behavior for linear polymer melts such as the tested iPPs). The Yao relaxation time is found to increase correctly with $M_w$, but its value is about one order of magnitude higher than the reptation-mode relaxation time, that is, on the order of milliseconds, which is interestingly the same order as the longest relaxation time for the given iPP. For example, the longest relaxation time for iPP with $M_w = 76$ kg/mol was found to be 5.36 ms at $230\,^{\circ}C$[20] and the Yao's relaxation time for the same material and temperature is 1.91 ms (see Table VI). The index of rotational recovery $n_0$ was found to be equal
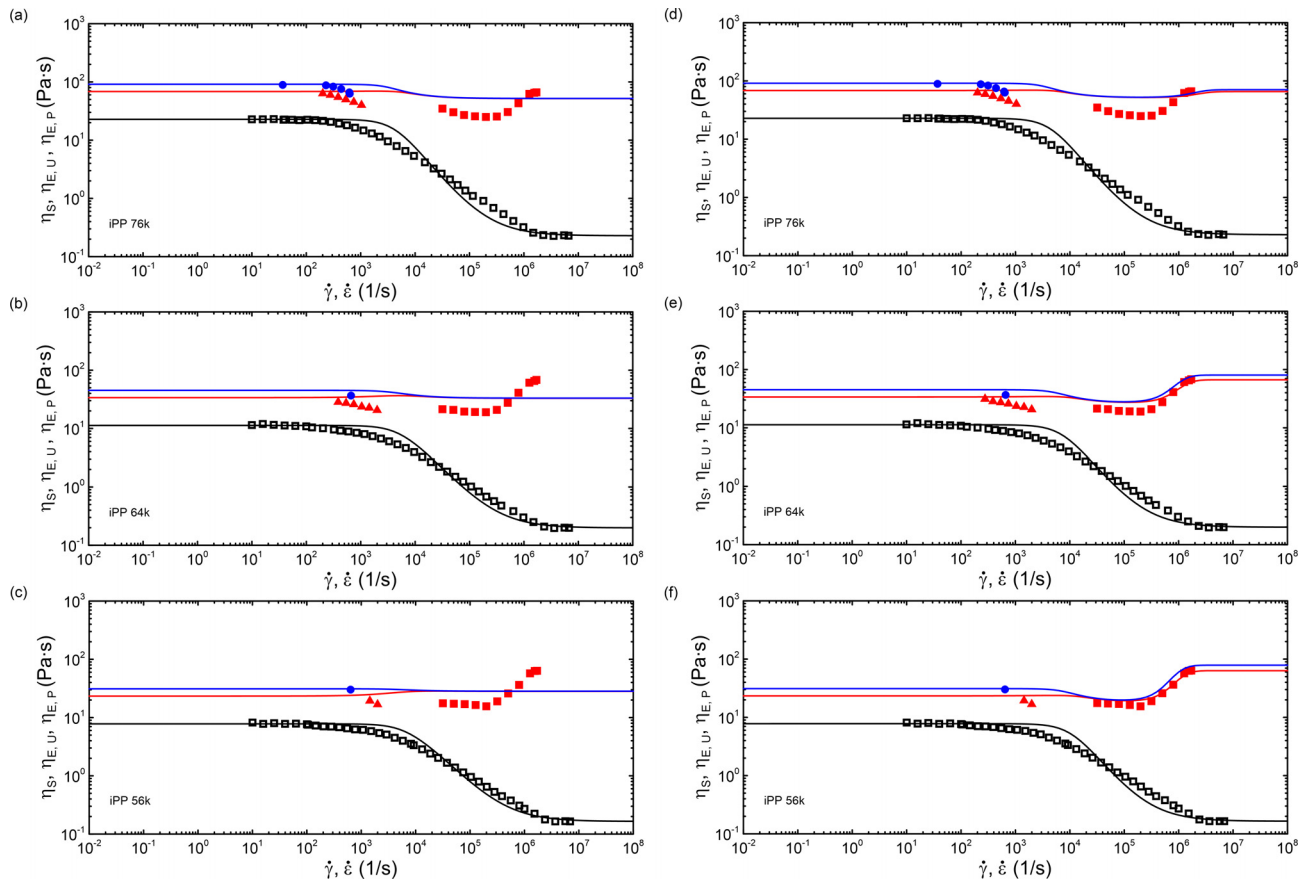
**FIG. 2.** Comparison between measured strain rate-dependent shear (open symbols), uniaxial (red full triangles and squares) and planar extensional viscosities (blue full circles), and model fits (curves) at 230 °C for three linear isotactic polypropylenes [76 k (a) and (d), 64 k (b) and (e), and 56 k (c) and (f)]. The original and modified single-mode Giesekus model predictions are shown in [(a)–(c)] and [(d)–(f)], respectively. Here, $\eta_S$ is the shear viscosity, $\eta_{E,U}$ is the uniaxial extensional viscosity, $\eta_{E,P}$ is the planar extensional viscosity, $\dot{\gamma}$ is the shear rate, and $\dot{\varepsilon}$ is the extensional strain rate.

to 1, independent of $M_w$, which is a typical value when no second normal stress difference, $N_2$, is available during the fitting procedure (in which case the model predicts $N_2 = 0$[28]). Yao pointed out that $n_0 > 1$ to correctly predict $N_2$. There is no simple relationship between the strain hardening coefficient $\psi$ and $M_w$ (see Table VI), which can be explained by the loss of physical meaning of $\psi$ due to the poor ability of the model to represent extensional viscosities at a very wide strain rate range.

The modified Yao model removes the shortcomings of the original Yao model, as can be deduced from Fig. 3 (right) and Table VII; that is, it correctly predicts both the occurrence of the secondary Newtonian plateau in the shear viscosity curve and the uniaxial and planar extensional viscosities over the entire strain rate range. Here, $\eta_0$, $\eta_\infty$, and $\eta_{E,U,\infty}$ parameters were taken from our previous work[19,21–23] (i.e., polymer viscosity $\eta_P$ is known in advance because $\eta_p = \eta_0 - \eta_\infty$), $S_0$ and $n_0$ were kept the same, equal to 1 as in the case of the original Yao model and remaining five parameters ($\lambda_P$, $\alpha_0$, $\psi$, $\lambda_2$, and $\beta$) were determined from the fit of shear, uniaxial, and planar extensional viscosities (see Table VII). As can be seen, the conclusions formulated for the Yao relaxation time $\lambda_P$ remain unchanged for the

modified version of the model and both strain hardening parameters $\psi$ and $\beta$ have a direct physical meaning as they both increase with reduced $M_w$ as expected.[44] $\lambda_2$ is of the same order as in the case of the mGNF model, but its value increases with decreasing $M_w$; that is, $\lambda_2$ is also inversely related to the Rouse time as in the case of the mGiesekus model.

It should be mentioned that the molecularized generalized Newtonian fluid (mGNF) constitutive equation as well as the explicit Yao model can only be used to model steady-state flows. On the other hand, the proposed modification (i.e., taking into account the role of the oligomeric solvent by replacing the commonly used Newton's law with a simplified mGNF equation in the fully viscoelastic constitutive equations) demonstrated here on the Giesekus model enables the modeling of transient flow types, since the extra-stress tensor in both the original and the modified Giesekus model is given as the sum of the time-dependent polymer stress and the time-independent stress contribution from the oligomeric solvent.

A second note is related to the high strain rate viscosity data (taken from Refs. 19 and 49), which are visualized in Figs. 1–3 together with the low strain rate data measured in this work. In our previous
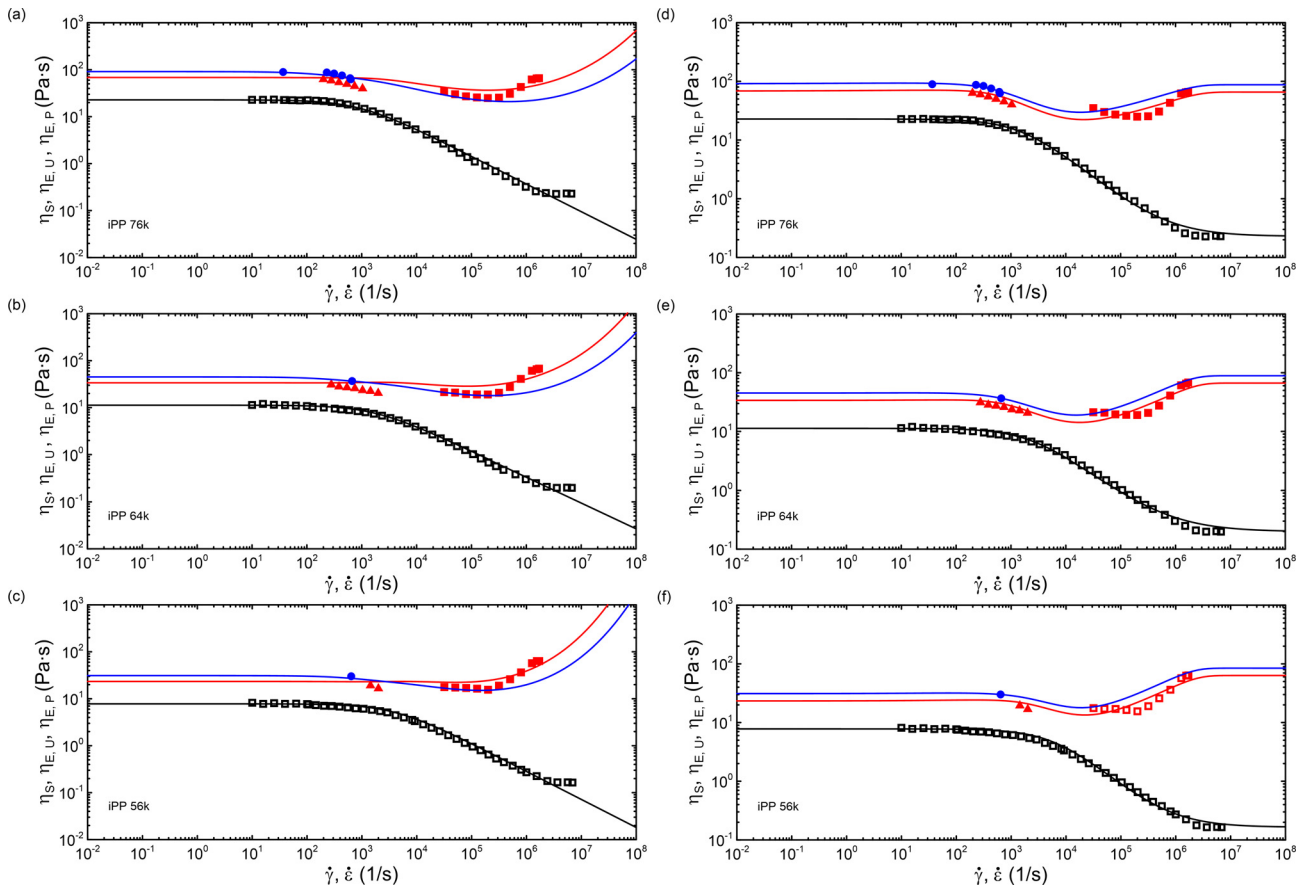
**FIG. 3.** Comparison between measured strain rate-dependent shear (open symbols), uniaxial (red full triangles and squares) and planar extensional viscosities (blue full circles), and model fits (curves) at 230 °C for three linear isotactic polypropylenes [76 k (a) and (d), 64 k (b) and (e), and 56 k (c) and (f)]. The original and modified explicit Yao model predictions are provided in [(a)–(c)] and [(d)–(f)], respectively. Here, $\eta_S$ is the shear viscosity, $\eta_{E,U}$ is the uniaxial extensional viscosity, $\eta_{E,P}$ is the planar extensional viscosity, $\dot{\gamma}$ is the shear rate, and $\dot{\varepsilon}$ is the extensional strain rate.

**TABLE III.** Parameters of the mGNF model.

| Sample name | $\eta_0$ (Pa s) | $\eta_\infty$ (Pa s) | $\lambda_1$ (s) | $a$ (−) | $n$ (−) | $\lambda_2$ (s) | $\beta$ (−) | $\eta_{E,U,\infty}$ (Pa s) | RMSE (−) |
|---|---|---|---|---|---|---|---|---|---|
| 76 k | 22.80 | 0.229 | 0.000 222 | 0.714 66 | 0 | $2.949 \times 10^{-7}$ | $2.25 \times 10^{-3}$ | 65.56 | 0.040 589 |
| 64 k | 11.27 | 0.199 | 0.000 101 | 0.644 10 | 0 | $2.850 \times 10^{-7}$ | $3.92 \times 10^{-3}$ | 66.62 | 0.035 214 |
| 56 k | 7.79 | 0.165 | 0.000 070 | 0.666 42 | 0 | $2.811 \times 10^{-7}$ | $5.74 \times 10^{-3}$ | 63.32 | 0.052 357 |

**TABLE IV.** Parameters of the single-mode original Giesekus model.

| Sample name | $\eta_P$ (Pa s) | $\eta_\infty$ (Pa s) | $\lambda$ (s) | $\alpha$ (−) | RMSE (−) |
|---|---|---|---|---|---|
| 76 k | 22.571 | 0.229 | 0.000 175 | 0.884 329 | 0.140 602 |
| 64 k | 11.071 | 0.199 | 0.000 134 | 0.684 022 | 0.127 962 |
| 56 k | 7.625 | 0.165 | 0.000 108 | 0.550 478 | 0.112 149 |

work, we demonstrated through finite element method (FEM) simulations that for the given iPP melts, die design used and experimental conditions, the effect of viscous dissipation and pressure canceled each other out (for more details, see the section "effect of viscous dissipation and pressure" in our previous paper[19]). We have shown that, first, the secondary Newtonian viscosity, $\eta_\infty$ (occurring above shear rates of $2 \times 10^6$ s$^{-1}$), depends linearly on the weight-averaged molecular weight, $M_w$, for both entangled linear and branched polypropylene melts, indicating that polymer chains became fully disentangled at the

**TABLE V.** Parameters of the single-mode modified Giesekus model.

| Sample name | $\eta_P$ (Pa s) | $\eta_\infty$ (Pa s) | $\lambda$ (s) | $\alpha$ (−) | $\lambda_2$ (s) | $\beta$ (−) | $\eta_{E,U,\infty}$ (Pa s) | RMSE (−) |
|---|---|---|---|---|---|---|---|---|
| 76 k | 22.571 | 0.229 | 0.000 171 | 0.894 346 | $2.692 \times 10^{-7}$ | 3.715 | 65.56 | 0.140 334 |
| 64 k | 11.071 | 0.199 | 0.000 102 | 0.870 280 | $6.113 \times 10^{-7}$ | 3.701 | 66.62 | 0.109 443 |
| 56 k | 7.625 | 0.165 | 0.000 071 | 0.876 304 | $7.054 \times 10^{-7}$ | 3.658 | 63.32 | 0.068 144 |

**TABLE VI.** Parameters of the original explicit Yao model.

| Sample name | $\eta_0$ (Pa s) | $\lambda_0$ (s) | $\psi$ (−) | $S_0$ (−) | $\alpha_0$ (−) | $n_0$ (−) | RMSE (−) |
|---|---|---|---|---|---|---|---|
| 76 k | 22.80 | 0.001 908 | 0.261 329 | 1 | 0.850 123 | 1 | 0.077 523 |
| 64 k | 11.27 | 0.001 042 | 0.286 876 | 1 | 0.836 304 | 1 | 0.064 623 |
| 56 k | 7.79 | 0.000 445 | 0.211 563 | 1 | 0.808 501 | 1 | 0.076 174 |

**TABLE VII.** Parameters of the modified explicit Yao model.

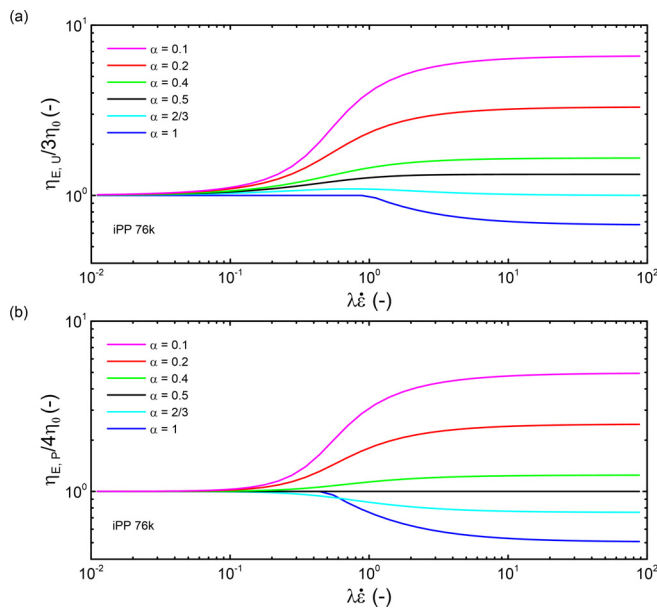| Sample name | $\eta_P$ (Pa s) | $\eta_\infty$ (Pa s) | $\lambda_P$ (s) | $\psi$ (−) | $S_0$ (−) | $\alpha_0$ (−) | $n_0$ (−) | $\lambda_2$ (s) | $\beta$ (−) | $\eta_{E,U,\infty}$ (Pa s) | RMSE (−) |
|---|---|---|---|---|---|---|---|---|---|---|---|
| 76 k | 22.571 | 0.229 | 0.001 044 | 2.464 340 | 1 | 3.250 488 | 1 | $2.172 \times 10^{-7}$ | $1.33 \times 10^{-9}$ | 65.56 | 0.049 322 |
| 64 k | 11.071 | 0.199 | 0.000 741 | 2.587 159 | 1 | 3.301 594 | 1 | $2.482 \times 10^{-7}$ | $5.82 \times 10^{-7}$ | 66.62 | 0.041 267 |
| 56 k | 7.625 | 0.165 | 0.000 259 | 2.786 014 | 1 | 3.626 322 | 1 | $2.528 \times 10^{-7}$ | $7.13 \times 10^{-7}$ | 63.32 | 0.045 144 |



**FIG. 4.** Effect of the anisotropic parameter $\alpha$ on the normalized uniaxial (a) and planar (b) extensional viscosities predicted by the Giesekus model for 76 k iPP melt at 230 °C.

secondary Newtonian plateau region. This conclusion was supported by the experimental observation that the high shear rate flow activation energy $E_\infty$ for the given PP melts is comparable to the zero-shear rate flow activation energy, $E_0$, of PP-like oligomer (squalane, $C_{30}H_{62}$; 2,6,10,15,19,23-hexamethyltetracosane).[19,49] Second, the free volume increases at the secondary Newtonian plateau due to complete chain disentanglement (most likely due to the coalescence of shaped free volume cavities), as indicated by a large change in the flow activation energies of PPs ($E_0 > E_\infty$).[19,49] Moreover, it was experimentally demonstrated by Takahashi *et al.*[50] that there is no wall slip at very high shear rates for PP at 230 °C (i.e., for the same polymer and flow conditions utilized in our work), which can also be explained by the complete chain disentanglements and significant increase in the free volume (i.e., no cohesive slip appears to occur and the adsorption force of the iPP chains to the wall surface appears to be high enough to suppress adhesive slip at very high strain rates).

## V. CONCLUSIONS

In this work, the Cogswell methodology was used to determine strain-rate-dependent planar and uniaxial extensional viscosities for various polypropylene melts using novel rectangular and circular orifice (zero-length) dies. The obtained experimental data were combined with shear and uniaxial extensional viscosity data determined at very high strain rates. The ability of the recently proposed mGNF constitutive equation to describe the measured data was shown to be very

high. The Giesekus and recently introduced explicit Yao viscoelastic constitutive equations were modified to include the effect of chemical environment (i.e., the role of the oligomeric solvent influencing the monomeric coefficient and extensional viscosities) using a simplified version of the mGNF constitutive equation for the solvent contribution to the stress tensor. The proposed generalization of Newton's law for an oligomeric solvent has been shown to significantly improve the ability of both constitutive equations to describe measured experimental data, especially at very high extensional strain rates using parameters with a clear physical meaning.

## ACKNOWLEDGMENTS

## AUTHOR DECLARATIONS

### Conflict of Interest

The authors have no conflicts to disclose.

### Author Contributions

**Jiří Drábek:** Formal analysis (equal); Investigation (equal); Methodology (equal); Visualization (lead); Writing – original draft (equal); Writing – review & editing (equal). **Martin Zatloukal:** Conceptualization (lead); Formal analysis (equal); Investigation (equal); Methodology (equal); Writing – original draft (equal); Writing – review & editing (equal).

## DATA AVAILABILITY

The data that support the findings of this study are available within the article.

## REFERENCES

[1]T. Barborik and M. Zatloukal, "Steady-state modeling of extrusion cast film process, neck-in phenomenon, and related experimental research: A review," Phys. Fluids **32**(6), 061302 (2020).

[2]Y. Demay and J. F. Agassant, "The polymer film casting process—An overview," Int. Polym. Process. **36**(3), 264–275 (2021).

[3]T. Barborik and M. Zatloukal, "Viscoelastic non-isothermal modeling of film extrusion for membrane production including flow induced crystallization," Phys. Fluids **34**(6), 063103 (2022).

[4]T. Barborik and M. Zatloukal, "Effect of heat transfer coefficient, draw ratio, and die exit temperature on the production of flat polypropylene membranes," Phys. Fluids **31**(5), 053101 (2019).

[5]S. Shiromoto, Y. Masutani, M. Tsutsubuchi, Y. Togawa, and T. Kajiwara, "The effect of viscoelasticity on the extrusion drawing in film-casting process," Rheol. Acta **49**(7), 757–767 (2010).

[6]S. Shiromoto, "The mechanism of neck-in phenomenon in film casting process," Int. Polym. Process. **29**(2), 197–206 (2014).

[7]T. Barborik, M. Zatloukal, and C. Tzoganakis, "On the role of extensional rheology and Deborah number on the neck-in phenomenon during flat film casting," Int. J. Heat Mass Transfer **111**, 1296–1313 (2017).

[8]T. Barborik and M. Zatloukal, "Effect of die exit stress state, Deborah number, uniaxial and planar extensional rheology on the neck-in phenomenon in polymeric flat film production," J. Non-Newtonian Fluid. Mech. **255**, 39–56 (2018).

[9]C. W. Macosko, *Rheology: Principles, Measurements, and Applications* (Wiley-VCH, New York, 1994).

[10]H. Münstedt, "Extensional rheology and processing of polymeric materials," Int. Polym. Process. **33**(5), 594–618 (2018).

[11]O. Hassager, Y. Wang, and Q. Huang, "Extensional rheometry of model liquids: Simulations of filament stretching," Phys. Fluids **33**(12), 123108 (2021).

[12]L. N. Jimenez, C. D. V. Martinez Narvaez, and V. Sharma, "Capillary breakup and extensional rheology response of food thickener cellulose gum (NaCMC) in salt-free and excess salt solutions," Phys. Fluids **32**(1), 012113 (2020).

[13]M. Zatloukal, "Extrusion head with inert flat slit of zero length," Czech patent 305409 (22 July 2015).

[14]M. Zatloukal, "Measurements and modeling of temperature-strain rate dependent uniaxial and planar extensional viscosities for branched LDPE polymer melt," Polymer **104**, 258–267 (2016).

[15]M. Zatloukal and J. Musil, "Analysis of entrance pressure drop techniques for extensional viscosity determination," Polym. Testing **28**(8), 843–853 (2009).

[16]M. Zatloukal and J. Musil, "Extrusion head with inert capillary of zero length," Czech patent 304382 (26 February 2014).

[17]F. N. Cogswell, "Converging flow of polymer melts in extrusion dies," Polym. Eng. Sci. **12**(1), 64–73 (1972).

[18]K. Walczak, M. Gupta, K. A. Koppi, J. Dooley, and M. A. Spalding, "Elongational viscosity of LDPEs and polystyrenes using entrance loss data," Polym. Eng. Sci. **48**(2), 223–232 (2008).

[19]J. Drabek, M. Zatloukal, and M. Martyn, "Effect of molecular weight on secondary Newtonian plateau at high shear rates for linear isotactic melt blown polypropylenes," J. Non-Newtonian Fluid Mech. **251**, 107–118 (2018).

[20]J. Drabek and M. Zatloukal, "Influence of long chain branching on fiber diameter distribution for polypropylene nonwovens produced by melt blown process," J. Rheol. **63**(4), 519–532 (2019).

[21]J. Drabek and M. Zatloukal, "Influence of molecular weight, temperature, extensional rheology on melt blowing process stability for linear isotactic polypropylene," Phys. Fluids **32**(8), 083110 (2020).

[22]M. Zatloukal and J. Drabek, "Reduction of monomeric friction coefficient for linear isotactic polypropylene melts in very fast uniaxial extensional flow," Phys. Fluids **33**(5), 051703 (2021).

[23]M. Zatloukal and J. Drabek, "Generalized Newtonian fluid constitutive equation for polymer liquids considering chain stretch and monomeric friction reduction for very fast flows modeling," Phys. Fluids **33**(8), 083106 (2021).

[24]M. Zatloukal, "Frame-invariant formulation of novel generalized Newtonian fluid constitutive equation for polymer melts," Phys. Fluids **32**(9), 091705 (2020).

[25]H. Giesekus, "A simple constitutive equation for polymer fluids based on the concept of deformation-dependent tensorial mobility," J. Non-Newtonian Fluid Mech. **11**(1–2), 69–109 (1982).

[26]H. Giesekus, "A unified approach to a variety of constitutive models for polymer fluids based on the concept of configuration-dependent molecular mobility," Rheol. Acta **21**(4–5), 366–375 (1982).

[27]H. Giesekus, "Stressing behaviour in simple shear flow as predicted by a new constitutive model for polymer fluids," J. Non-Newtonian Fluid Mech. **12**(3), 367–374 (1983).

[28]D. Yao, "An explicit non-Newtonian fluid model for polymeric flow with finite stretch," in Annual Technical Conference—ANTEC, Conference Proceedings, Charlotte, NC June 14–16 (2022).

[29]M. Zatloukal, J. Vlcek, C. Tzoganakis, and P. Saha, "Improvement in techniques for the determination of extensional rheological data from entrance flows: Computational and experimental analysis," J. Non-Newtonian Fluid Mech. **107**(1–3), 13–37 (2002).

[30]M. Padmanabhan and C. W. Macosko, "Extensional viscosity from entrance pressure drop measurements," Rheola. Acta **36**(2), 144–151 (1997).

[31]R. Drouot and M. Lucius, "Second-order approximation of the law of behavior of simple fluids. Classical laws deduced by the introduction of a new objective tensor," Arch. Mech. Stosow. **28**(2), 189–198 (1976).

[32]R. Drouot, "Définition d'un transport associé à un modè de fluide du deuxième ordre. comparison de diverses lois de comportement," C.R. Acad. Sci. Paris, Ser. A **282**, 923–926 (1976).

[33]G. Astarita, "Objective and generally applicable criteria for flow classification," J. Non-Newtonian Fluid Mech. **6**(1), 69–76 (1979).

[34]D. Yao, "A non-Newtonian fluid model with an objective vorticity," J. Non-Newtonian Fluid Mech. **218**, 99–105 (2015).

[35]D. Yao, "A non-Newtonian fluid model with finite stretch and rotational recovery," J. Non-Newtonian Fluid Mech. **230**, 12–18 (2016).

[36]G. Ianniruberto, G. Marrucci, and Y. Masubuchi, "Melts of linear polymers in fast flows," Macromolecules **53**(13), 5023–5033 (2020).

[37]J. M. Dealy, D. J. Read, and R. G. Larson, *Structure and Rheology of Molten Polymers: From Structure to Flow Behavior and Back Again*, 2nd ed. (Hanser, Munich 2018).

[38]R. G. Larson, *Constitutive Equations for Polymer Melts and Solutions* (Butterworths, Boston, 1988).

[39]R. B. Bird, *Dynamics of Polymeric Liquids* 2nd ed. (John Wiley, New York, 1987).

[40]Q. Huang, N. J. Alvarez, Y. Matsumiya, H. K. Rasmussen, H. Watanabe, and O. Hassager, "Extensional rheology of entangled polystyrene solutions suggests importance of nematic interactions," ACS Macro Lett. **2**(8), 741–744 (2013).

[41]Q. Huang and H. K. Rasmussen, "Stress relaxation following uniaxial extension of polystyrene melt and oligomer dilutions," J. Rheol. **60**(3), 465–471 (2016).

[42]G. Ianniruberto, "Extensional flows of solutions of entangled polymers confirm reduction of friction coefficient," Macromolecules **48**(17), 6306–6312 (2015).

[43]G. W. Park and G. Ianniruberto, "Flow-induced nematic interaction and friction reduction successfully describe PS melt and solution data in extension startup and relaxation," Macromolecules **50**(12), 4787–4796 (2017).

[44]R. G. Larson and P. S. Desai, "Modeling the rheology of polymer melts and solutions," Annu. Rev. Fluid Mech. **47**, 47–65 (2015).

[45]J. M. Wiest, "A differential constitutive equation for polymer melts," Rheol. Acta **28**(1), 4–12 (1989).

[46]V. R. Iyengar and A. Co, "Film casting of a modified Giesekus fluid: Stability analysis," Chem. Eng. Sci. **51**(9), 1417–1430 (1996).

[47]M. E. Pis-Lopez and A. Co, "Multilayer film casting of modified Giesekus fluids Part 1. Steady-state analysis," J. Non-Newtonian Fluid Mech. **66**(1), 71–93 (1996).

[48]V. R. Iyengar and A. Co, "Film casting of a modified Giesekus fluid: A steady-state analysis," J. Non-Newtonian Fluid Mech. **48**(1–2), 1–20 (1993).

[49]J. Drabek, M. Zatloukal, and M. Martyn, "Effect of molecular weight, branching and temperature on dynamics of polypropylene melts at very high shear rates," Polymer **144**, 179–183 (2018).

[50]H. Takahashi, T. Matsuoka, and T. Kurauchi, "Rheology of polymer melts in high shear rate," J. Appl. Polym. Sci. **30**(12), 4669–4684 (1985).